J. Plasma Fusion Res. SERIES, Vol. 8 (2009)

Electron Acceleration by Oscillating Electric Field

Akira TSUSHIMA and Osamu ISHIHARA

Faculty of Engineering, Yokohama National University, Yokohama 249-8501, Japan

(Received: 6 September 2008 / Accepted: 14 January 2009)

A unique experimental system with collisionless electrons has been developed to investigate wave-particle interaction and/or particle acceleration in turbulence. In the system, electrons are injected from a tip of electron source along a magnetic field in a region between two electrostatic potentials. Some of the electrons trapped in the potentials are accelerated and other electrons are decelerated by oscillating electric field localized at the electrostatic potential with larger magnitude. The accelerated electrons were observed as a current into a disk electrode placed outside the steady electrostatic potential with lower magnitude. The results show that the escaping electrons' current was the superposition of (1) current enhanced at some discrete frequencies of the oscillating electric field and (2) current continuously increased with increasing the frequency of the oscillating electric field.

Keywords: electron acceleration, stochastic acceleration, wave-particle interaction, bounce motion

1. Introduction

Cosmic ray particles with extremely high energy range between 10^8 eV and 10^{21} eV have been observed [1] and a power law distribution in the medium energy range has been explained by a diffusive shock acceleration model at supernova. The model is based on Fermi acceleration, the original of which was the acceleration by particle scattering against moving magnetic inhomogeneities [2].

In laboratory plasmas, Fermi acceleration has been investigated in relation to wave-particle interactions or interactions between electric field and electrons from the wave viewpoint [3, 4, 5] and from the particle viewpoint [6, 7, 8]. Subsequently, the experiment of electron heating has been performed in an electron trap, where oscillating electric fields interacted with bouncing electrons [9]. Similar work was reported in the past in an after glow plasma as a model experiment of the transit time heating based on Fermi acceleration [10]. In these experiments, electrons were thermalized due to frequent electron collisions.

In the present experiment, electrons were injected along magnetic field from a tip of electron source and trapped between two electrostatic potentials [11, 12], which were apart by a distance of $L \simeq 30$ cm. Since the trapped electron density was approximately 1×10^7 cm^{-3} under a back ground pressure of $p \lesssim 10^{-4}$ Pa, the electron was able to move back and forth approximately 10^4 times between the two electrostatic potentials and the collisionless condition was satisfied [12]. Then, by applying an oscillating electric field to one of the electrostatic potentials, the electron acceleration related to the resonance of the electron bounce motion was observed and that related to stochastic nature was also observed. These results are different from the previous results [11, 12] due to the resonance of the transmission line for the oscillating electric field. The problem of the resonance was removed by terminating the transmission line in the characteristic impedance of 50 Ω in the present experiment.

author's e-mail: tsushima@ynu.ac.jp

2. Experimental Setup

Electrons were injected in a trap consisting of cylindrical electrodes with an inner diameter of 20 mm along a magnetic field with an intensity of $B = 440$ G by a tip of heated LaB_6 (DENKA Electron Emitter, M3 IS) placed almost on the axis of the central electrode as shown in Fig. 1 (a). The trap was set in a vacuum vessel (base pressure: $p \simeq 3 \times 10^{-5}$ Pa) and the magnetic field was carefully adjusted to be directed along the axis of the central electrode and the plug electrodes (A) and (B), by two sets of correction coils, which produced magnetic fields with the directions perpendicular to the axial direction, i.e., the vertical and horizontal directions. In the result, the accuracy of the direction of the magnetic field was $\lesssim 10^{-4}$. In this figure, bias potentials V_A and V_B to the plug electrodes (A) and (B), respectively, generate the two electrostatic potentials and the electrons from the electron emitter with the acceleration potential of V_E are trapped between two electrostatic potentials. Since the axial length of the plug electrodes is much larger than the inner diameter, the maximum absolute values on the electrostatic potentials (A) and (B) are almost the values of $|V_A|$ and $|V_B|$, respectively. In fact, the potential profile on the axis such as shown in Fig. 1 (b) is formed for the typical values of $V_A = -80$ V and $V_B = -60$ V. The dotted line represented in Fig. 1 (b) corresponds to the value of $V_E = -30$ V and its intersections with the solid curve, which represents the axial potential profile, indicate the reflection points of an electron from the electron emitter. Then, an oscillating electric field was applied by introducing a RF signal with a frequency f_A up to 50 MHz to the plug electrode (A). The transmission line of the RF

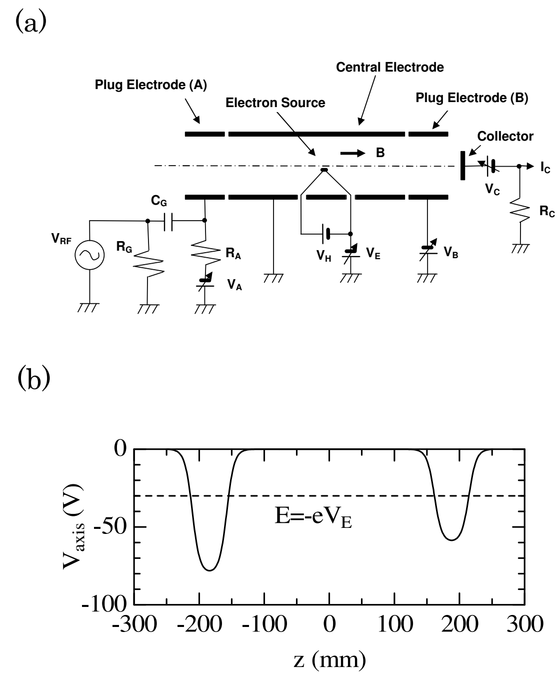

Fig. 1 (a) Schematic of experimental setup and (b) axial potential profile, where $V_A = -80$ V, $V_B = -60$ V, $V_E = -30$ V, $V_H = 1.8$ V, $V_C = 1.5$ V, $C_G = 0.1$ μF, $R_G = 50$ Ω, $R_A = 1.6$ kΩ, $R_C = 10$ kΩ, and $B = 440$ G in the typical conditiion.

signal was terminated in the characteristic impedance of $R_G = 50$ Ω and passed through the capacitance of $C_G = 0.1$ μF to the plug electrode (A) so that the problem of the resonance of the transmission line was removed. In the experiment, the amplitude of the RF signal, $\tilde{V}_{\rm RF}$, was varied up to 10 V. The amplitude of the potential oscillation at the reflection point of the electron with an energy of E can be estimated by

$$\tilde{V}_{\rm reflect} \simeq \tilde{V}_{\rm RF}\ \frac{E}{(-eV_A)}\ ,$$

since the oscillating potential profile at the electrode (A) always keeps a similar shape, where e is the elementary charge. For example, $\tilde{V}_{\rm reflect} \simeq 3.75$ V for an electron with the injection energy of $E = -eV_E = 30$ eV when $\tilde{V}_{\rm RF} = 10$ V and $V_A = -80$ V.

In the system, some of the electrons between the two electrostatic potentials (A) and (B) are accelerated or decelerated when the electrons are reflected at the electrostatic potential (A) with the oscillating electric field. The electrons reached sufficiently high energy by successive acceleration can escape from the electrostatic potential (B), the magnitude of which is less than that of the electrostatic potential (A), i.e., $|V_B| < |V_A|$. Then, the escaping electrons are detected as a current of $I_{\rm C}$ by the collector placed farther right of the plug electrode (B), as shown in Fig. 1 (a), and the increase of the kinetic energy of the escaping electrons from its initial kinetic energy is easily evaluated by

$$\Delta K \geq -e(V_B - V_E)\ .$$

3. Results

Figure 2(a) shows the current I_C, due to the escaping electrons through the electrostatic potential (B), as a function of time t when the frequency f_A of the oscillating electric field was swept between 1 and 50 MHz, which is represented by a sweep voltage $V_{\rm sweep}$ as a function of time t in Fig. 2(b) under the condition of $V_A = -80$ V, $V_B = -60$ V, $V_E = -30$ V, and $\tilde{V}_{RF} \simeq 7.5$ V. Figure 3 shows the relationship between the current I_C and the frequency f_A, which is obtained from Figs. 2(a) and (b). In Fig. 3, four peaks of I_C can be easily found and their frequencies are approximately 39.5, 42.6, 44.9, and 47.2 MHz. Besides the peak with the lowest frequency of 39.5 MHz, the difference between the two adjacent frequencies is ~ 2.2 MHz, which agrees with the bounce frequency of an electron with a kinetic energy of ~ 4.8 eV. Since the density of the electron cloud between the two electrostatic potentials were estimated to be approximately 1×10^7 cm^{-3} and the space potential on the axis of the central electrode to be approximately -25 V, the value of ~ 4.8 eV may be considered as the initial kinetic energy K_0 of the electrons from the electron emitter: $K_0 \sim 4.8$ eV. In fact, the difference of the adjacent peak frequencies was inversely proportional to the axial length L of the two electrostatic potentials. In that case, the gain of the kinetic energy of the escaping electron can be estimated as

$$A = \frac{\Delta K}{K_0} \gtrsim 6.3\ .$$

If we see Fig. 3 carefully, then, we find that the base of I_C continuously increases with increasing f_A for $f_A \gtrsim 40$ MHz. So, we may say that the current I_C is composed of (1) current enhanced at some discrete frequencies of the oscillating electric field and (2) current continuously increased with increasing the frequency of the oscillating electric field.

By the variation of $\tilde{V}_{\rm RF}$, the relationship between I_C and f_A varies, as shown in Fig. 4, where the upper, middle, and lower curves represent the cases of $\tilde{V}_{\rm RF} =$ 10, 7.5, and 5 V, respectively, under the condition of $V_A = -80$ V, $V_B = -60$ V, and $V_E = -30$ V. This figure shows that the magnitude of I_C increases with increasing $\tilde{V}_{\rm RF}$; and the discretely enhanced current of the type (1) is clearer for the case of the smaller $\tilde{V}_{\rm RF}$ and the continuously increasing current of the type (2) is clearer for the case of the larger $\tilde{V}_{\rm RF}$.

The relationships between I_C and f_A for various values of V_B are also shown in Fig. 5 under the condition of $V_A = -80$ V, $V_E = -30$ V, and $\tilde{V}_{\rm RF} = 7.5$ V. Here, the upper, middle, and lower curves represent

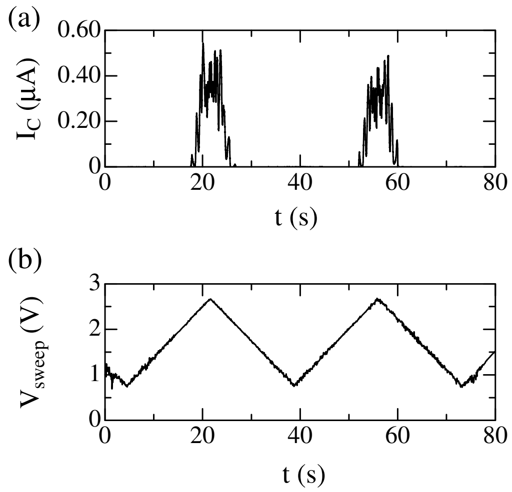

Fig. 2 (a) Current I_C as a fuction of time t and (b) sweep voltage $V_{\rm sweep}$, corresponding to f_A, as a function of time t under the condition of $V_A = -80$ V, $V_B = -60$ V, $V_E = -30$ V, and $\tilde{V}_{RF} \simeq 7.5$ V.

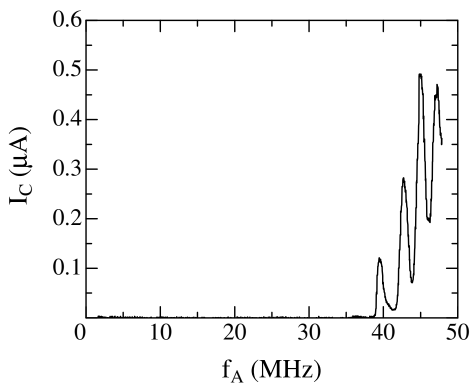

Fig. 3 Relationship between current I_C and frequency f_A, which is obtained from Figs. 2(a) and (b).

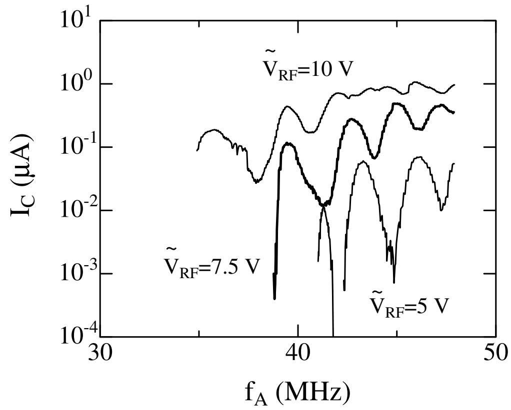

Fig. 4 Relationships between I_C and f_A for $\tilde{V}_{RF} = 10$, 7.5, and 5 V, which are represented by upper, middle, and lower curves, respectively, under the condition of $V_A = -80$ V, $V_B = -60$ V, and $V_E = -30$ V.

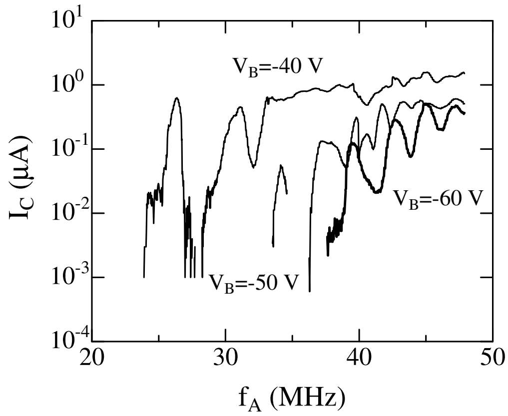

Fig. 5 Relationships between I_C and f_A for $V_B = -40$, -50, and -60 V, which are represented by upper, middle, and lower curves, respectively, under the condition of $V_A = -80$ V, $V_E = -30$ V, and $\tilde{V}_{\rm RF} = 7.5$ V.

the cases of $V_B = -40$, -50, and -60 V, respectively. From the figure, we can see that the magnitude of I_C decreases with increasing $|V_B|$; and the discretely enhanced current of the type (1) is clearer for the case of the larger $|V_B|$ and the continuous increasing current of the type (2) is clearer for the case of the smaller $|V_B|$.

Figure 6 shows the relationship betweem I_C and f_A under the condition of $V_A = -80$ V, $V_B = -40$ V, $V_E = -30$ V, and $\tilde{V}_{\rm RF} = 10$ V. From the discussion of Figs. 4 and 5, it is considered that the continuous increasing current of the type (2) appears clear in Fig. 6. In fact, the base of I_C becomes large and the ratio of the magnitude of the peak and that of the base for $f_A \gtrsim 40$ MHz is $\lesssim 1.3$, which is smaller than the ratio of $\gtrsim 2.5$ in the case of $V_A = -80$ V, $V_B = -60$ V, $V_E = -30$ V, and $\tilde{V}_{\rm RF} = 7.5$ V (Fig. 3). In the frequency range of $f_A < 40$ MHz of Fig. 6, some peaks of I_C appear and the ratios of the magnitude of the peaks and that of the base are relatively large (> 2), although the rate of the electron acceleration is very small and I_C was not observed in the case of $V_A = -80$ V, $V_B = -60$ V, $V_E = -30$ V, and $\tilde{V}_{\rm RF} = 7.5$ V (Fig. 3). Thus, with the fact that the difference of the frequencies of the adjacent peaks was inversely proportional to L, we see that the electron acceleration rate increased around the frequencies with the peaked I_C due to the resonance of the elec-

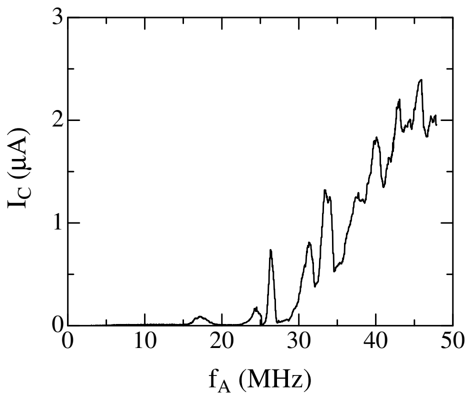

Fig. 6 Relationship between I_C and f_A under the condition of $V_A = -80$ V, $V_B = -40$ V, $V_E = -30$ V, and $\tilde{V}_{\rm RF} = 10$ V.

tron bounce motion; and we observed as the discretely enhanced current of the type (1). On the other hand, the continuous increasing current of the type (2), or the base of I_C increased with increasing the frequency of f_A, would be related to the stochastic nature of the electron acceleration.

4. Summary

We have investigated the electron acceleration under the collisionless condition by the oscillating electric field in the system, where electrons were injected from a tip of electron source along the magnetic field between the two electrostatic potentials. The oscillating electric field was localized at the electrostatic potential with larger magnitude and accelerated some of the electrons trapped between the two electrostatic potentials. Then, the sufficiently accelerated electrons were observed as the current into the disk electrode placed outside the steady electrostatic potential with lower magnitude. The results show that the escaping electron current was the superposition of (1) the current enhanced at some discrete frequencies of the oscillating electric field and (2) the continuously increasing current with increasing the frequency of the oscillating electric field. It can be considered that the discretely enhanced current of the type (1) was related to the electron bounce motion and the continuously increasing current of the type (2) was to the electron's stochastic nature.

The experiments with the oscillating electric field with different two or three frequencies have been performed to investigate particle acceleration in turbulence.

[1] J. W. Cronin, Rev. Mod. Phys. **71**, S165 (1999).
[2] E. Fermi, Phys. Rev. **75**, 1169 (1949).
[3] A. Y. Wong, N. D'Angelo, and R. W. Motley, Phys. Rev. Lett. **9**, 415 (1962).
[4] H. Derfler and T. C. Simon, Phys. Rev. Lett. **17**, 172 (1966).
[5] J. H. Malmberg and C. B. Wharton, Phys. Rev. Lett. **17**, 175 (1966).
[6] F. Doveil, Phys. Rev. Lett. **46**, 532 (1981).
[7] F. Skiff, F. Anderegg, and N. Q. Tran, Phys. Rev. Lett. **58**, 1430 (1987).
[8] H. Shoyama, M. Y. Tanaka, S. Higashi, Y. Kawai, and M. Kono, J. Phys. Soc. Jpn. **65**, 2860 (1996).
[9] B. P. Cluggish, J. R. Danielson, and C. F. Driscoll, Phy. Rev. Lett. **81**, 353 (1998).
[10] H. Sugai, K. Ido, and S. Takeda, J. Phys. Soc. Jpn. **46**, 228 (1979).
[11] A. Tsushima, and O. Ishihara, Proc. 25th Int. Conf. Phenomena Ionized Gases (Nagoya, 2001) Vol.1, pp. 347.
[12] A. Tsushima and O. Ishihara, Proc. 11th Int. Cong. Plasma Phys. (Sydney, 2002) pp.125.